BONE

Wnt1 is an Lrp5-independent bone-anabolic Wnt ligand

Julia Luther[1]*, Timur Alexander Yorgan[1]*, Tim Rolvien[1]*, Lorenz Ulsamer[1], Till Koehne[1,2], Nannan Liao[1], Daniela Keller[1†], Nele Vollersen[1], Stefan Teufel[1‡], Mona Neven[1], Stephanie Peters[1], Michaela Schweizer[3], Andreas Trumpp[4], Sebastian Rosigkeit[5], Ernesto Bockamp[5], Stefan Mundlos[6,7,8], Uwe Kornak[6,7,8], Ralf Oheim[1], Michael Amling[1§], Thorsten Schinke[1§], Jean-Pierre David[1§]

WNT1 **mutations in humans are associated with a new form of osteogenesis imperfecta and with early-onset osteoporosis, suggesting a key role of WNT1 in bone mass regulation. However, the general mode of action and the therapeutic potential of Wnt1 in clinically relevant situations such as aging remain to be established. Here, we report the high prevalence of heterozygous *WNT1* mutations in patients with early-onset osteoporosis. We show that inactivation of Wnt1 in osteoblasts causes severe osteoporosis and spontaneous bone fractures in mice. In contrast, conditional Wnt1 expression in osteoblasts promoted rapid bone mass increase in developing young, adult, and aged mice by rapidly increasing osteoblast numbers and function. Contrary to current mechanistic models, loss of Lrp5, the co-receptor thought to transmit extracellular WNT signals during bone mass regulation, did not reduce the bone-anabolic effect of Wnt1, providing direct evidence that Wnt1 function does not require the LRP5 co-receptor. The identification of Wnt1 as a regulator of bone formation and remodeling provides the basis for development of Wnt1-targeting drugs for the treatment of osteoporosis.**

INTRODUCTION

Bone remodeling is a postdevelopmental physiological process occurring throughout life that is required to ensure bone regeneration and long-term stability of the skeleton. This process is initiated by the bone-embedded osteocytes that act as mechanical sensors of bone microdamage, which promote the differentiation and recruitment of osteoclasts to resorb the mineralized bone matrix and activate osteoblasts to secrete and mineralize new bone matrix (*1*–*3*). A fraction of osteoblasts remains trapped within the newly formed bone, where they differentiate into osteocytes that will secrete inhibitors of osteoblastogenesis to terminate the remodeling cycle (*1*, *2*). The balance between bone resorption and formation is essential to maintain skeletal integrity, and any disturbance in this balance will lead to the development of bone pathologies, the most common being postmenopausal osteoporosis in aging women with drastic consequences on their quality of life, increased fracture incidence, and mortality (*4*, *5*). Osteoporosis is mainly treated with antiresorptive drugs such as bisphosphonates (*6*). However, blocking bone resorption interrupts the normal coupling of bone remodeling, thereby also causing inhibition of de novo bone formation (*7*). Over the long term, this has detrimental consequences for bone quality and can cause serious adverse effects such as osteonecrosis of the jaw, atypical bone fractures, and modification of hematopoietic cell niches (*8*, *9*). Anabolic drugs targeting bone formation by activating osteoblasts would be preferable because such therapies would not block bone remodeling (*5*). Intermittent injection of parathyroid hormone fragment (PTH; also called teriparatide) is the main bone-anabolic drug used clinically. However, its application is limited because of the mode of delivery requiring daily injections for 24 months, high cost, and the risk of osteosarcoma induction as seen in rat models (*10*, *11*). More promising bone-anabolic drugs are under development, most of which target natural inhibitors of the essential osteoblastogenic WNT [wingless-type mouse mammary tumor virus (MMTV) integration site family] signaling pathway (*3*).

Initially deduced from the identification of high bone mass mutations in humans, the bone-anabolic function of WNT signaling was further validated in mice. These mutations cause either a gain of function of the WNT co-receptor low-density lipoprotein receptor–related protein 5 (LRP5) or a loss of function of its inhibitor Sclerostin (SOST) (*3*, *12*, *13*). The mutated proteins act at the level of the WNT signaling receptor complex that consists of a member of the Frizzled family as well as co-receptors from the LRP family. The combination of extracellular WNT ligands with specific receptors can lead to the activation of different cellular signal transduction cascades generally categorized into β-catenin–based canonical and Jun kinase or Ca^{2+} signaling noncanonical pathways. Although the known gain- and loss-of-function phenotypes suggested a role of canonical WNT signaling as a regulator of bone formation, this has not been firmly demonstrated. For example, inactivation of β-catenin, the essential downstream cotranscription factor of canonical WNT signaling, provided contrasting information in mouse models. Loss of β-catenin in early mesenchymal progenitors favored chondrogenic differentiation of these cells at the expense of osteoblastogenesis (*14*, *15*), whereas inactivation in committed osteoblasts demonstrated the role of β-catenin in mediating the repression of osteoclastogenesis via induction of osteoprotegerin (OPG) expression in osteoblasts (*16*). In addition, although canonical WNT signaling directly

[1]Department of Osteology and Biomechanics, University Medical Center Hamburg-Eppendorf, 20246 Hamburg, Germany. [2]Department of Orthodontics, University Medical Center Hamburg-Eppendorf, D 20246 Hamburg, Germany. [3]Center for Molecular Neurobiology Hamburg, University Medical Center Hamburg-Eppendorf, D 20251 Hamburg, Germany. [4]Division of Stem Cells and Cancer, Deutsches Krebsforschungszentrum (DKFZ), D 69120 Heidelberg, Germany. [5]Institute for Translational Immunology and Research Center for Immunotherapy, University Medical Center, Johannes Gutenberg University, D 55131 Mainz, Germany. [6]Institute of Medical Genetics and Human Genetics, Charité-Universitätsmedizin Berlin, D 13353 Berlin, Germany. [7]Berlin-Brandenburg Center for Regenerative Therapies, Charité-Universitätsmedizin Berlin, D 13353 Berlin, Germany. [8]Max Planck Institute for Molecular Genetics, D 14195 Berlin, Germany.
*These authors contributed equally to this work.
†Present address: Berlin-Brandenburg Center for Regenerative Therapies, Charité-Universitätsmedizin Berlin, D 13353 Berlin, Germany.
‡Present address: Institute of Experimental Musculoskeletal Medicine, Medical Faculty of the University of Münster, D 48149 Münster, Germany.
§Corresponding author. Email: j.david@uke.de (J.-P.D.); schinke@uke.de (T.S.); amling@uke.de (M.A.)

inhibits osteoclastogenesis and therefore bone resorption rather than increasing bone formation (*17*, *18*), the activation of the noncanonical pathway appeared to positively regulate both bone formation and bone resorption (*19*–*21*). However, the occurrence of wingless-type mouse mammary tumor virus (MMTV) integration site family, member 1 (*WNT1*) mutations in a new form of osteogenesis imperfecta and in early-onset osteoporosis strongly suggest that WNT1 is a key regulator of bone formation in humans (*22*–*24*), a hypothesis subsequently reinforced in mice carrying a hypomorphic Wnt1 mutation (*25*) and with Dmp1-*cre*–mediated conditional *Wnt1* deletion (*26*). Given the potential off-target recombination reported using the Dmp1-*cre* line (*27*), the cellular source of Wnt1 is still unclear.

Thus, two key questions remain to be solved: the first regarding the cellular source of Wnt1 that acts as a bone-anabolic stimulus and the second regarding whether Wnt1 is acting via the Sost/Lrp5 pathway to induce bone formation. Given the global function of WNT signaling during development, in tissue homeostasis, and in tumor formation, answering these questions is fundamental to the design of clinically applicable agonist molecules that can stimulate bone formation without dangerous and unwanted side effects. Using genetically modified mouse models, we report the bone-anabolic function of Wnt1 when produced by osteoblasts. We also demonstrate that this Wnt1 bone-anabolic activity does not require Lrp5 function. Our study thus provides important new insights into the mechanisms governing bone homeostasis and establishes Wnt1 as a natural bone-anabolic molecule with the potential for treating osteoporosis and other low bone mass pathologies.

RESULTS

Humans carrying *WNT1* mutations have high fracture incidence and low bone turnover

To confirm the causative role of *WNT1* mutations in bone fragility in humans, we analyzed 83 patients diagnosed with early-onset osteoporosis [dual-energy x-ray absorptiometry (DXA) *T* score < −2.5; age <50 years] by mutational enrichment using a custom-designed SureSelectXT gene panel containing all coding exons of 373 genes associated with changes in bone mass, skeletal dysplasias, dysostosis, or connective tissue diseases [skeletal disorder–associated genome (sDAG)]. This analysis revealed pathogenic mutations in the *WNT1* gene of seven patients (8.5%). A subsequent segregation analysis identified a family with specific *WNT1* mutations in four likewise affected relatives (Fig. 1A). Of these 11 patients with early-onset osteoporosis, 9 had a history of low-traumatic fractures. Vertebral and nonvertebral fractures were observed with a frequency increasing with age (Fig. 1, A and B). DXA revealed a Z score < −2.0 at the lumbar spine or hip in seven adult cases, indicating an overall reduction in areal bone mineral density (Fig. 1, C and D). Seven of 9 (78%) of the adult patients were diagnosed with osteoporosis according to the World Health Organization criteria (*T* score < −2.5). High-resolution peripheral quantitative computed tomography (HR-pQCT) at the distal tibia and at the distal radius revealed a combined trabecular and cortical bone loss, with a slightly more pronounced reduction in cortical thickness than in trabecular parameters when compared to controls from published reference values (Fig. 1, E to H, and fig. S1, A to D) (*28*, *29*). We performed histomorphometric analysis on undecalcified sections of an iliac crest biopsy (Fig. 1I) of one of the adult patients (case #3 in Fig. 1A) that revealed decreased structural parameters and low osteoblast and osteoclast numbers and surfaces (Fig. 1J), suggesting a pathology that is caused by low bone turnover. Analysis of the serum parameters for bone turnover in all patients at initial presentation showed relatively low quantity of two markers for bone formation, namely osteocalcin and bone-specific alkaline phosphatase (BAP), compared to reference ranges from our local laboratory (University Medical Center Hamburg-Eppendorf). In these patients, deoxypyridinoline (DPD) per creatinine measured in the urine revealed no increased bone resorption, confirming a low bone turnover state (Fig. 1, K to M). Last, we analyzed the evolution of the bone turnover markers in the serum and urine of a patient with history of multiple fractures receiving a sequential treatment with denosumab and teriparatide, which indicated a correction of the low bone turnover state in response to teriparatide (Fig. 1, N to P), resulting in complete prevention of fractures for more than 5 years (Fig. 1Q). Thus, heterozygous *WNT1* mutations can be considered as one of the most frequent mutations in patients with early-onset osteoporosis associated with a high incidence of low-traumatic fractures due to low bone turnover.

Osteoblast-targeted Wnt1 inactivation in mice phenocopies bone defects associated with *WNT1* mutations in humans

To provide direct evidence for the role of Wnt1 in bone metabolism, we took advantage of a mouse line carrying floxed alleles of *Wnt1* ($Wnt1^{fl/fl}$) (Fig. 2A). Because *Wnt1* expression has been reported in both osteoblasts and osteoclasts (*23*, *30*), we crossed the $Wnt1^{fl/fl}$ mice with *Runx2-Cre* mice (to inactivate Wnt1 in the osteoblastic lineage) or with *Lyz2-Cre* mice (to delete Wnt1 in the monocytic lineage, including the osteoclasts). Genotyping confirmed the lineage-specific recombination of the *Wnt1* allele in bones with the *Runx2-Cre* deleter line (Fig. 2B) as well as the efficacy of in vivo recombination using the *Lyz2-Cre* line (fig. S2A). Bone marrow–derived mesenchymal progenitors cultured ex vivo under osteoblastogenic conditions confirmed the efficacy of *Runx2-Cre*–mediated recombination in the osteoblast lineage (Fig. 2B). Similarly, the efficacy of *Lyz2-Cre*–mediated recombination in osteoclasts was confirmed in ex vivo generated osteoclasts (fig. S2A). No obvious bone phenotype could be observed when targeting Wnt1 inactivation in monocytes (fig. S2, B to E). To address the role of Wnt1 in osteocytes, we generated *Dmp1-Cre;*$Wnt1^{fl/fl}$ mice from which no clear conclusive data about the cellular origin of Wnt1 could be drawn due to recombination events observed in multiple tissues (fig. S3A). However, fractures were observed in all *Runx2-Cre;*$Wnt1^{fl/fl}$ mice analyzed by x-ray at the age of 24 weeks (Fig. 2C), and these mice developed multiple fractures as shown by micro–computed tomography (μCT) imaging (Fig. 2, D and E). The presence of callus observed in von Kossa–, toluidine blue–, or Masson-Goldner–stained sections further confirmed that fractures occurred in multiple locations in *Runx2-Cre;*$Wnt1^{fl/fl}$ mice (fig. S3, B and C). These analyses also revealed a decreased trabecular bone volume and cortical thickness in femora not affected by fractures (Fig. 2, F to H) as well as an increased fragility in a three-point bending test (Fig. 2I). This phenotype was not linked to decreased circulating Wnt1 in the deleter mice (fig. S3D), suggesting a local mode of action of Wnt1 in bone. Thus, general osteoporosis with high bone fragility develops in the absence of Wnt1 expression in the osteoblast lineage but not upon *Wnt1* deletion in monocytes. The generalized osteoporosis in *Runx2-Cre;*$Wnt1^{fl/fl}$ mice phenocopies the pathology found in patients with *WNT1* mutations and provides direct experimental proof that Wnt1 loss of function in osteoblasts is responsible for this condition.

Fig. 1. Characteristics of patients with heterozygous *WNT1* mutations. (**A**) Number of patient demographics: sex, age, genotype, and fracture history [Vert. Fx (*n*), number of vertebral fractures; Per. Fx (*n*), peripheral fractures] of all patients. (**B**) Radiographies showing typical fractures of the spine (left), distal femur (middle), and proximal femur (right) in patients (numbers 1, 3, 5). Arrows point to the fracture lines. (**C**) DXA measurement (Z scores) at the lumbar spine and (**D**) at the hip. (**E**) HR-pQCT at the distal tibia. (**F**) Table of mean values of bone parameters and percent change compared to controls (% ref) at the distal tibia (in bold are the most affected parameters). Tb.N, trabecular number; Tb.Th, trabecular thickness; Ct.Th, cortical thickness. (**G** and **H**) Age-related changes of bone volume per tissue volume (BV/TV) and cortical thickness (Ct.Th) at the distal tibia. (**I**) Trichrome-Goldner staining of an iliac crest biopsy from patient 3. Scale bars, 1 mm (left) and 50 µm (right). (**J**) Bone histomorphometry of the biopsy. Tb.Sp, trabecular separation; O.Th, osteoid thickness; OS/BS, osteoid surface per bone surface; OV/BV, osteoid volume per bone volume; Ob.S/BS, osteoblast surface per bone surface; Oc.S/BS, osteoclast surface per bone surface. (**K**) Serum osteocalcin and (**L**) BAP measured in all patients at initial presentation compared to the reference range (gray boxes). (**M**) DPD per creatinine measured in the urine. (**N** to **P**) Evolution of bone parameters in patient 1 over 6-year treatment with denosumab and teriparatide, (N) osteocalcin, (O) BAP, and (P) DPD and (**Q**) timeline (years) showing the clinical history. Gray boxes indicate the reference range for each parameter.

A

Number	Sex	Age	Mutation	Vert. Fx (*n*)	Per. Fx (*n*)
1	F	78	p.Arg235Trp	9	3
2	M	46	p.Arg235Trp	1	>20
3	F	52	p.Arg235Trp	0	1
4	M	7	p.Arg235Trp	0	0
5	F	9	p.Arg235Trp	0	1
6	F	28	p.Val117Gly	0	0
7	M	42	p.Val117Gly/ p.Asp244Tyr	0	>20
8	M	32	p.Arg235Trp	0	1
9	F	63	p.Gly252Arg	5	1
10	F	44	p.Gly162Alafs*37	0	3
11	M	56	c.624G>A (splicing)	2	>20

B

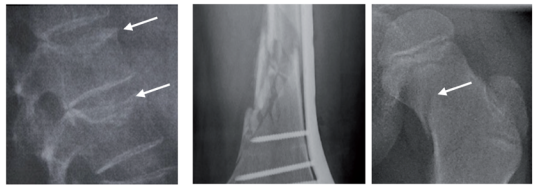

C

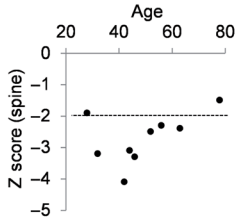

D

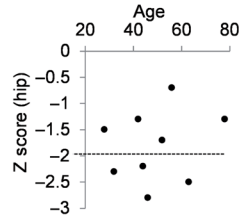

E

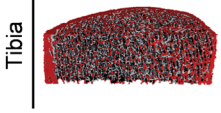

F

Parameter	Mean ± SD (%ref)
BV/TV (%)	11.98 ± 3.5 **(74.6)**
Tb.N (1/mm)	1.82 ± 0.4 (95.2)
Tb.Th (mm)	0.065 ± 0.009 (76.8)
Ct.Th (mm)	0.62 **(49.4)**

G

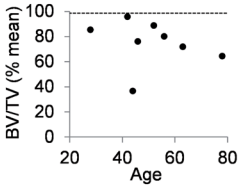

H

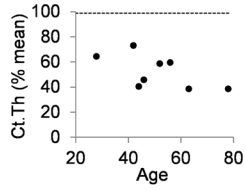

I

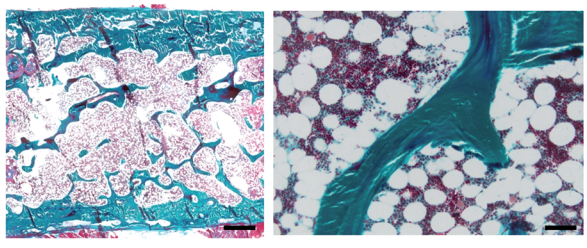

J

Parameter	Value
BV/TV (%)	12.4
Tb.N (1/mm)	0.97
Tb.Th (µm)	127.2
Tb.Sp (µm)	898.5
O.Th (µm)	13.7
OS/BS (%)	15.4
OV/BV (%)	3.2
Ob.S/BS (%)	3.6
Oc.S/BS (%)	1.4

K

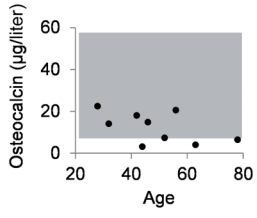

L

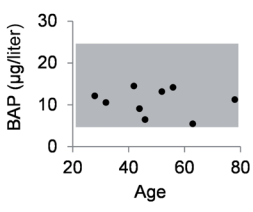

M

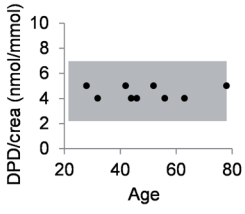

N

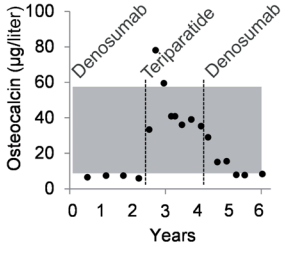

O

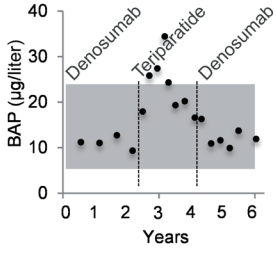

P

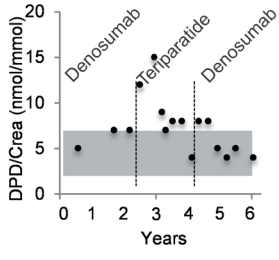

Q

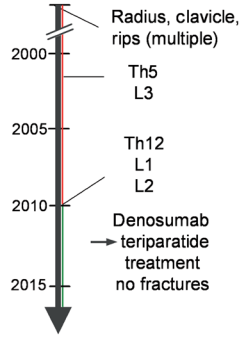

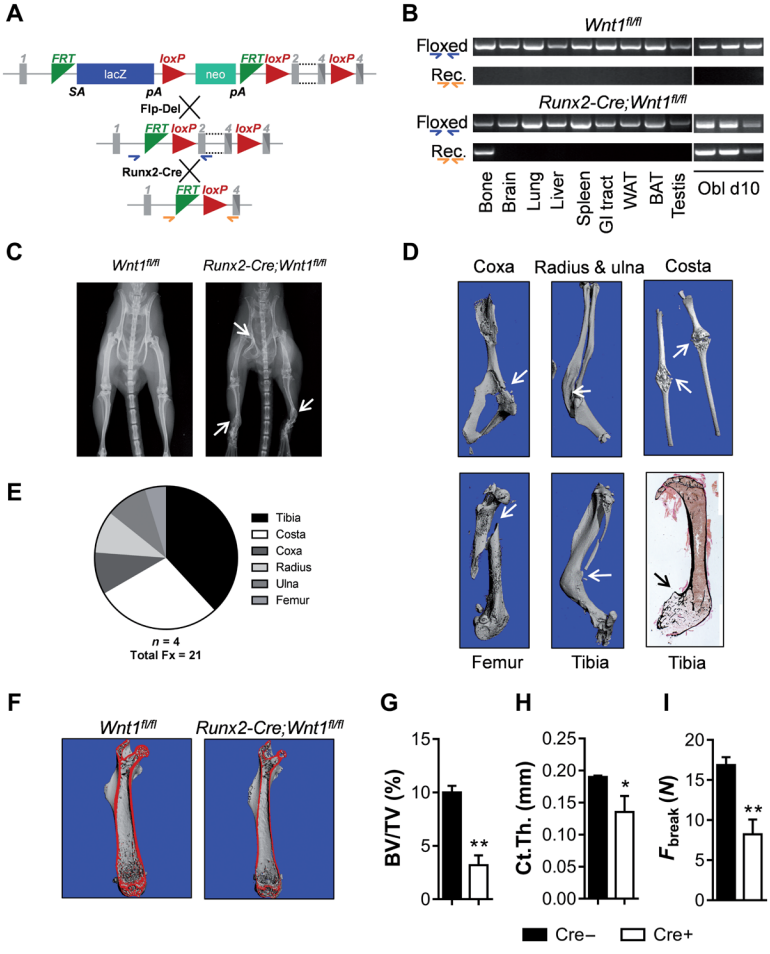

Fig. 2. Wnt1 inactivation in osteoblasts phenocopies *WNT1* mutations in humans. (**A**) Strategy used to generate *Wnt1* conditional deletion. The localization of the primers used for genotyping is indicated by the blue arrows for the floxed and by the orange arrows for the recombined alleles. (**B**) Genotyping of various tissues isolated from mice homozygote for the *Wnt1* floxed allele intercrossed or not with the *Runx2-Cre* deleter. Genotyping of bone marrow–derived osteoblasts is shown. (**C**) X-ray of 24-week-old *Wnt1*$^{fl/fl}$ and *Runx2-Cre;Wnt1*$^{fl/fl}$ male littermates; the arrows indicate the presence of fractures. (**D**) µCT scan of the indicated bones and von Kossa staining of the tibia of *Runx2-Cre;Wnt1*$^{fl/fl}$; the arrows indicate the presence of fractures. (**E**) Frequency distribution of the fractures in the various bones of 24-week-old *Runx2-Cre;Wnt1*$^{fl/fl}$ mice. $n = 4$ mice carrying a total of 21 detectable fractures (Fx). (**F**) Longitudinal section of µCT-scanned femora of *Wnt1*$^{fl/fl}$ and *Runx2-Cre;Wnt1*$^{fl/fl}$. (**G**) Quantification of the trabecular BV/TV and (**H**) of the cortical thickness. (**I**) Force necessary to fracture femurs as determined by three-point bending test. $n = 4$ (*Wnt1*$^{fl/fl}$) and $n = 3$ (*Runx2-Cre;Wnt1*$^{fl/fl}$) for (G) to (I). Data are the means ± SEM. $^{**}P < 0.01$; $^{*}P < 0.05$ (unpaired *t* test).

Wnt1 is rapidly induced in an osteoblast-targeted transgenic mouse model

To mechanistically characterize the effect of Wnt1 production by osteoblasts for regulating bone mass, we made use of an osteoblast-targeted inducible *Wnt1* transgenic mouse model (hereafter called *Wnt1*Tg). In this model, doxycycline (DOX)–dependent *Wnt1* transgene expression is governed by the *Col1a1* promoter-driven tetracycline-controlled transcriptional activator (*Col1a1-tTA*), resulting in conditional *Wnt1* expression in cells expressing *Col1a1*, including osteoblasts in the bone, upon DOX withdrawal (Fig. 3A). To confirm transgene induction, we first compared the expression of *Wnt1* mRNA in long bones and calvariae of 6-week-old *Wnt1*Tg mice and controls (any mice lacking one or both transgenes) 2 days after DOX withdrawal to *Wnt1* mRNA expression in mice permanently receiving DOX. As expected, upon DOX withdrawal, *Wnt1* mRNA expression was markedly increased in long bones and calvariae of *Wnt1*Tg animals but not in control mice (Fig. 3B). Expression was not affected by removing DOX from the food in littermate controls, and we did not observe any significant differences in *Wnt1* expression between the uninduced controls and not-induced *Wnt1*Tg mice (Fig. 3B). Thus, *Wnt1* transgene activation is fast and tightly regulated. To further address the tissue specificity of the transgene expression, we compared the *Wnt1* mRNA expression in various tissues of 6-week-old *Wnt1*Tg and control mice 1 week after DOX removal. Whereas the spleen, gut, long bone, and calvaria of control mice had elevated *Wnt1* expression (Fig. 3C), *Wnt1* mRNA was further increased in the flushed bone, bone marrow, and calvaria and, to some extent, also in the spleen and gut of transgenic mice. By contrast, *Wnt1* mRNA remained unchanged in all other tissues tested (Fig. 3D). Permanent transgene activation in 3-week-old *Wnt1*Tg animals resulted in a time-dependent increase in circulating Wnt1 protein in the sera of transgenic mice, 3 and 9 weeks after induction (Fig. 3E). Low expression of Wnt1 was detected by immunostaining in bone lining cells of the control mice, and increased expression in the same cells was observed in transgenic mice after 1 week of induction (Fig. 3F). Increased bone density was revealed by x-ray of *Wnt1*Tg mice that had been induced for 9 weeks (Fig. 3G). These data demonstrate that the *Wnt1* transgene can be rapidly induced in osteoblastic cells and that this induction leads to the synthesis of a functional Wnt1 ligand, resulting in increased bone mass.

Trabecular and cortical bone mass increase in *Wnt1* transgenic mouse

We next compared histological sections of undecalcified spines and tibiae from the induced transgenic mice to age- and sex-matched control littermates or to the not-induced transgenic mice. Increased trabecular bone volume and cortical thickness were observed by von Kossa staining of the sections from the 6-week-old males 3 weeks after transgene induction (Fig. 4A). The increased trabecular volume was further confirmed by quantitative histomorphometry of 6-week-old mice (3 weeks after induction of the transgene) as well as in 12-week-old mice (9 weeks after induction of the transgene), revealing a significant ($^{****}P < 0.0001$) increase in trabecular bone volume (BV/TV) (Fig. 4B), higher trabecular thickness (Fig. 4C), and increased trabecular numbers (Fig. 4D). Very similar effects were observed in females, demonstrating that the bone-anabolic effect of Wnt1 is gender independent (fig. S4A). No changes in bone parameters were observed in the two control groups, excluding any effects promoted by DOX. Similarly, no differences were observed between *Wnt1* transgenic and non-transgenic mice maintained under constant DOX administration, demonstrating tight transgene regulation (Fig. 4, B to D). The increased trabecular bone volume, trabecular numbers, and trabecular thickness were confirmed by µCT analysis of the femoral bone (Fig. 4E and fig. S4, B and C), as was the time-dependent increase in cortical thickness (Fig. 4, E and F, and fig. S4B). Increased bone density in the

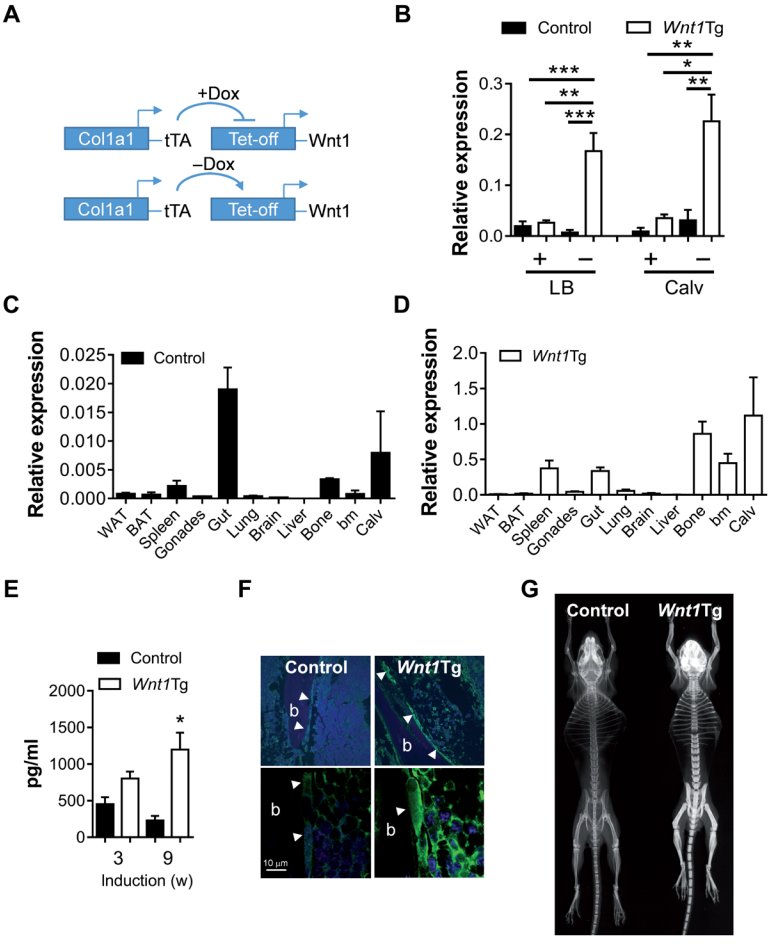

Fig. 3. The inducible Tet-off *Wnt1* transgene is functional. (**A**) Schematization of the Tet-off system used to generate the transgenic mice. The tTA driver is controlled by the *Col1a1* promoter gene to regulate the expression of *Wnt1* transgene in the osteoblastogenic lineage. *Wnt1* expression is silenced in the presence of DOX (+Dox) and induced when removing it (–Dox) from the food. (**B** to **D**) Quantitative real-time fluorescence polymerase chain reaction (QPCR) analysis of *Wnt1* expression (B) in long bones (LB) and calvariae (Calv) of 6-week-old male control or *Wnt1* transgenic (*Wnt1*Tg) mice 2 days after removing the DOX (–) compared to littermates maintained with DOX (+) ($n \geq 3$) and in various organs of 6-week-old control (C) or *Wnt1*Tg (D) males after removing DOX for 1 week [note that the *y*-axis scales differ between (C) and (D); $n \geq 2$]. WAT, white adipose tissue; BAT, brown adipose tissue; bm, bone marrow; Calv, calvariae. (**E**) Enzyme-linked immunosorbent assay (ELISA) quantification of circulating Wnt1 in control and *Wnt1*Tg males 3 weeks (3) and 9 weeks (9) after DOX removal, starting from the age of 3 weeks (w). $n = 3$. (**F**) Low (top) and high (bottom) magnification of Wnt1 immunostaining in tibiae of 6-week-old control and *Wnt1*Tg mice 1 week after DOX removal; white arrowheads indicate the presence of osteoblasts lining trabecular bone (b). (**G**) X-ray of 12-week-old control and *Wnt1*Tg male mice (9 weeks after DOX removal). Data are the means ± SEM. ***$P < 0.001$; **$P < 0.01$; *$P < 0.05$ [unpaired *t* test (E) or one-way analysis of variance (ANOVA) (B)].

calvariae of *Wnt1*-expressing mice was also evident as shown by μCT imaging and von Kossa staining (fig. S4, D and E). Transgene activation induced the closure of cranial sutures (fig. S4, D and E), a phenotype usually associated with increased osteoblast activity. Thus, switching on *Wnt1* expression for 3 and 9 weeks in growing mice markedly increased bone mass in trabecular, cortical, and intramembranous bone.

Increasing Wnt1 expression stimulates bone formation

To gain insight into the cellular mechanism driving Wnt1-promoted increased bone mass, we performed histomorphometry on toluidine blue–stained undecalcified spine sections of 12-week-old mice (Fig. 5A). Although no differences between the osteoclast numbers per bone perimeter and the osteoclast surface per bone surface occurred after Wnt1 activation (Fig. 5, B and C), *Wnt1* expression promoted significantly increased osteoblast numbers (*$P < 0.05$) and osteoblast surface per bone surface (*$P < 0.05$) (Fig. 5, D and E). Analysis of spine sections after in vivo double calcein labeling suggested a marked increase in the amount of newly formed bone (Fig. 5F) and a higher mineral apposition rate (MAR) (Fig. 5G) in Wnt1-induced mice, which was confirmed by dynamic histomorphometric quantification. We observed a tendency to an increased mineralizing surface per bone surface as well as a significantly higher MAR (**$P < 0.01$) in the Wnt1-induced cohort, resulting in a doubled bone formation rate (BFR) (Fig. 5, H to J). These data demonstrate that inducing Wnt1 in growing mice does not affect bone resorption but rather augments bone formation by increasing the number and activity of osteoblasts.

Wnt1 has bone-anabolic activity in adult and aging mice

Having shown that inducing *Wnt1* expression increases bone mass by stimulating bone formation in young growing mice with intense bone modeling, we next asked whether similar effects would be seen in adult mice in a phase of active bone remodeling after reaching their bone mass peak. We first induced *Wnt1* expression for 3 weeks in young adults, starting at 12 weeks of age. Transgene activation resulted in increased bone mass in the 15-week-old mice as shown by von Kossa staining of undecalcified sections of the vertebrae and tibiae (fig. S5A). These observations were further confirmed by histomorphometry of the spine, demonstrating an increased bone mass due to higher trabecular numbers and thickness (fig. S5B). μCT analysis of the femora of the induced *Wnt1*Tg mice confirmed the increased trabecular bone volume caused by higher trabecular numbers and thickness as well as the increased cortical thickness (fig. S5, C to E). Directly in line with these findings, induced *Wnt1*Tg mice had an increased resistance to fracture in the three-point bending test (fig. S5F). Again, although osteoclast parameters were unaffected by *Wnt1* expression (fig. S5G), the increased bone mass was associated with higher osteoblast numbers and surface area (fig. S5H), and a markedly increased BFR (fig. S5I). Similar results were obtained when analyzing the bone of 6-month-old females after inducing *Wnt1* transgene expression for 4 weeks (fig. S6). These findings demonstrate that the osteoanabolic potential of Wnt1 is also present in mice that have reached their bone mass peak and that this effect is gender independent.

Because Wnt1 is a strong bone-anabolic molecule in adult mice, Wnt1-agonist strategies may represent a powerful approach for treating postmenopausal and senile osteoporosis. To further test this possibility, we induced Wnt1 expression in 1-year-old female mice and performed a complete skeleton analysis. Again, an increase in bone mass was observed in the spine when inducing Wnt1 in these older mice (Fig. 6, A and B). This phenotype was associated with increased osteoblastogenesis without any effect on osteoclastogenesis (Fig. 6, C and D), leading to a net-increased BFR (Fig. 6E). The increased bone mass was observed in all bones including the endochondral

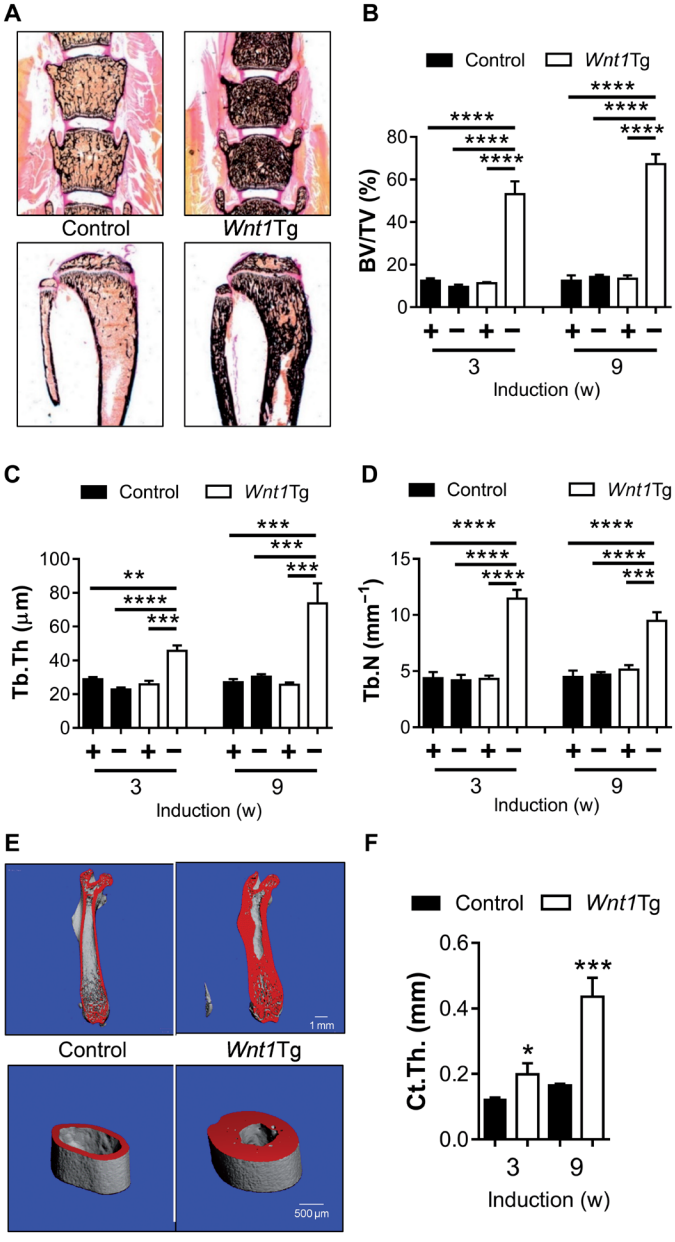

Fig. 4. High bone mass is induced when switching on *Wnt1* in growing mice. (**A**) von Kossa staining of vertebrae and tibiae of 6-week-old control and *Wnt1Tg* male mice after removing DOX for 3 weeks. (**B** to **D**) Histomorphometric analysis of the trabecular bone parameters of 6-week-old mice after removing DOX for 3 weeks (–) compared to mice kept under DOX (+). The same analysis was performed in 12-week-old mice after inducing the transgene for 9 weeks. $n \geq 3$. (B) Bone volume per tissue volume (BV/TV). (C) Trabecular thickness (Tb.Th). (D) Trabecular numbers (Tb.N). (**E**) Representative μCT of longitudinal (top panels) and of transversal sections at midshaft (bottom panels) scans of femora of 12-week-old control and *Wnt1* transgenic mice 9 weeks after removing DOX. (**F**) Quantification of cortical thickness in 6-week-old mice 3 weeks after removing the DOX or in 12-week-old mice 9 weeks after induction. $n \geq 4$. Data are the means ± SEM. ****$P < 0.0001$; ***$P < 0.001$; **$P < 0.01$; *$P < 0.05$ [one-way ANOVA (B to D) or unpaired *t* test (F)].

bones as illustrated by the increased trabecular and cortical bone of the femurs (Fig. 6, F to I), as well as in the intramembranous bone of the calvaria (Fig. 6, J and K). These analyses demonstrated the powerful general bone-anabolic property of Wnt1 in aging mice, a relevant model for aging-related osteoporosis.

Increase in bone mass after Wnt1 expression is rapid

The rapid induction of Wnt1 expression detected 2 days after DOX removal (Fig. 3B) allowed for investigation into whether a rapid increase in bone mass takes place after transgene induction, a phenomenon that would be highly desirable for therapeutic applications. To test this possibility, we induced transgene expression for 1 week in 5-week-old mice and saw that bone mass was markedly increased after 1 week of induction (Fig. 7, A and B). Under these experimental conditions, the phenotype was not associated with an increase in circulating Wnt1 (Fig. 7C), excluding the possibility that the bone-anabolic function of Wnt1 is caused by a systemic effect. Again, osteoclast numbers or surface area remained stable (Fig. 7D), whereas osteoblast numbers and surface area increased (Fig. 7E). To determine whether the observed rapid increase in bone mass was only limited to young, still growing animals with highly active bone modeling, we repeated the experiment in adult mice (30 weeks old). Similar results were obtained upon transgene expression in adult mice (fig. S7, A to D), indicating a general and age-independent bone-anabolic Wnt1 mode of action. These data provide direct in vivo evidence that Wnt1, by increasing osteoblast numbers, is a fast and robust bone-anabolic molecule in both growing and adult mice. To further confirm these observations, we performed QPCR analysis for markers of osteoblast differentiation 2 and 7 days after switching on transgene expression. We verified the strong induction of *Wnt1* mRNA that was already detectable 2 days after induction (Fig. 7F). In line with the rapidly increased osteoblast number, the expression of markers for bone formation were all increased in a time-dependent manner in the bone of the induced *Wnt1* transgenic mice (Fig. 7G). When analyzing the expression of WNT/β-catenin target genes, some but not all known potential target genes were significantly regulated (*$P < 0.05$) in response to Wnt1, including cyclin D1 (*Ccnd1*); Wnt inhibitory factor 1 (*Wif1*); WNT1-inducible signaling pathway protein 1 (*Wisp1*); gap junction protein, alpha 1 (*Gja1*); lipocalin 2 (*Lcn2*); and thrombospondin 1 (*Thbs1*), but not *OPG* (*Tnfrsf11b*) and *Rankl* (*Tnfsf11*) (Fig. 7H). Adenomatosis polyposis coli down-regulated 1 (*Apcdd1*), a known negative regulator of WNT signaling (*31*), was the most strongly induced gene and was already significantly increased 2 days after stimulation (*$P < 0.05$). No obvious changes in the expression of any components of the Hippo/WNT signaling cascade were detected (fig. S7E), suggesting that noncanonical WNT signaling is not involved in the regulation of Wnt1-induced bone formation.

Induction of increased bone mass is not due to an autocrine stimulation of osteoblast differentiation

To mechanistically characterize the phenotype at the cellular level, we compared the differentiation of primary osteoblasts isolated from the calvariae of neonatal transgenic mice with cells isolated from littermate control pups. We confirmed the increased expression of *Wnt1* after DOX withdrawal from the media (fig. S8A). Although not secreted in the media (fig. S8B), the increased protein expression in response to DOX removal was detected by Western blotting (fig. S8C). However, alizarin red staining at the end of the differentiation process did not indicate increased generation of bone nodules (fig. S8, D to E). In agreement, no increase in the expression

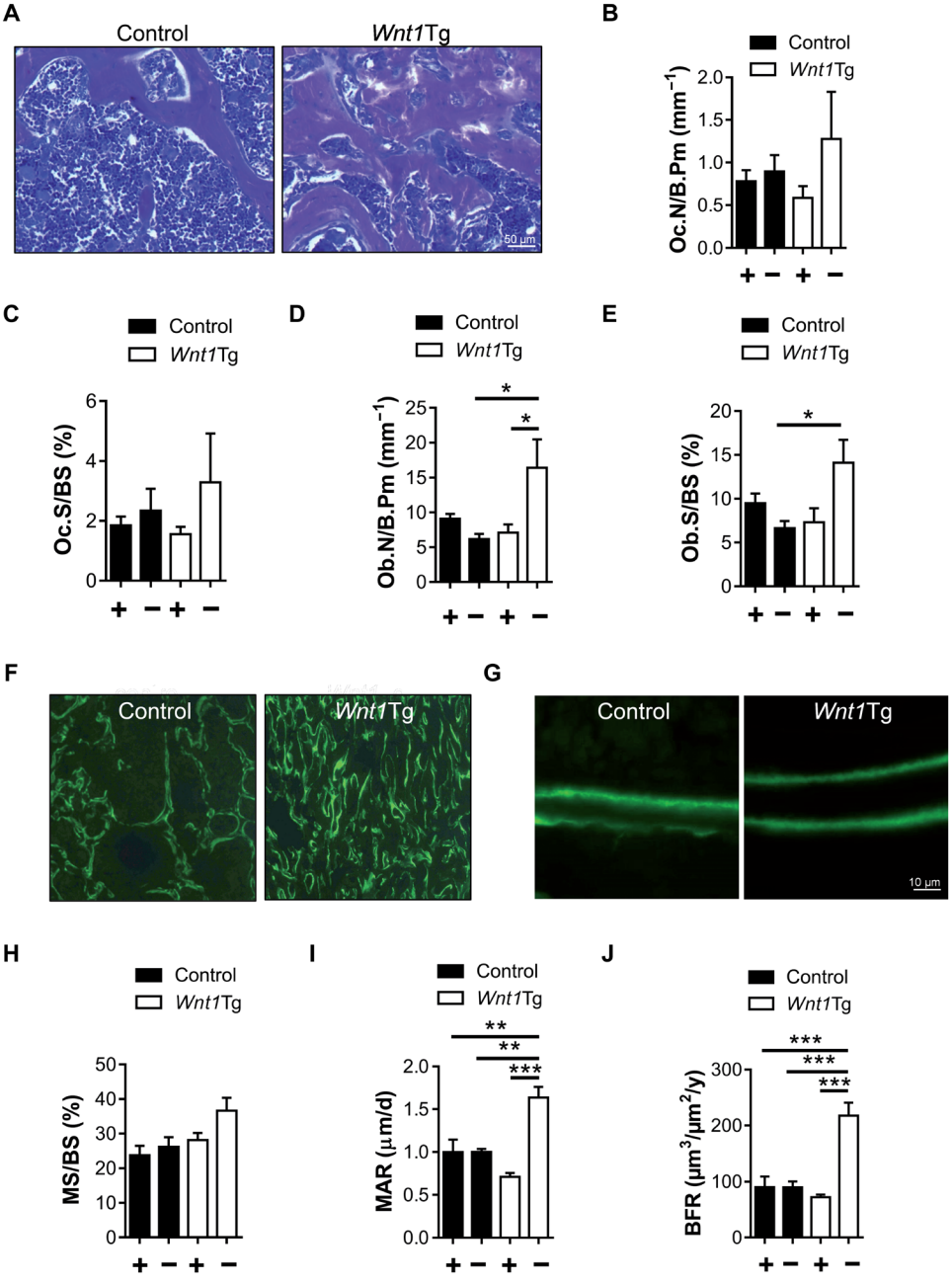

Fig. 5. Wnt1 is a bone-anabolic Wnt ligand. (**A**) Representative toluidine blue staining of vertebral sections of 12-week-old male mice after removing DOX for 9 weeks. (**B** to **E**) Histomorphometric analysis of the cellular components of the bones after removing DOX for 9 weeks (–) compared to mice kept under DOX (+). (B) Osteoclast numbers per bone perimeter (Oc.N/B.Pm). (C) Osteoclast surface area per bone surface (Oc.S/BS). (D) Osteoblast numbers per bone perimeter (Ob.N/B.Pm). (E) Osteoblast surface area per bone surface (Ob.S/BS). (**F**) Representative low-magnification and (**G**) high-magnification calcein double labeling of sections of the vertebrae of 12-week-old control and *Wnt1*Tg, 9 weeks after removing the DOX. (**H** to **J**) Dynamic histomorphometry analysis of (H) mineralizing surface per bone surface, (I) MAR, and (J) BFR in the 12-week-old mice, 9 weeks after inducing the transgene. $n \geq 3$. Data are the means ± SEM. ***$P < 0.001$; **$P < 0.01$; *$P < 0.05$ (one-way ANOVA).

of markers for osteoblast differentiation was detected when inducing the transgene (fig. S8F). The only obvious change among osteoblast markers was a significant inhibition of *Sost* and bone gamma carboxyglutamate protein (*Bglap*) expression (*$P < 0.05$), confirming the known repression of the latter gene by WNT signaling (*32*). The functionality of the transgene was also confirmed by increased *Axin2* expression. Again, consistent with the in vivo data, *Apcdd1* was found significantly up-regulated (*$P < 0.05$) (fig. S8F). Western blot analysis indicated that mTORC1 (mammalian target of rapamycin complex 1) pathway activation was unaffected, as shown by the unchanged S6 phosphorylation (fig. S8G). We further investigated the kinetic of expression of *Wnt1* in primary osteoblast cultures isolated from wild-type mice and could not find a time-dependent variation during the course of differentiation, including during the late stage of differentiation when osteocyte marker gene expression increased (fig. S9). Thus, although being active and modulating gene transcription, Wnt1 expression, which is not regulated during osteoblast differentiation, does not induce bone formation by directly increasing the capacity of primary osteoblast to differentiate.

Wnt1-induced increased bone mass is independent of Lrp5

On the basis of the bone phenotype in humans carrying gain-of-function mutation in *LRP5* (*33*) and the genetic analysis of Lrp5 gain or loss of function in mice (*27*, *34*, *35*), it is generally accepted that the recruitment of LRP5 as a co-receptor for frizzled proteins mediates downstream bone-anabolic activity of WNT ligands, although this has not been shown experimentally. We therefore generated *Lrp5*-deficient *Wnt1*Tg mice and saw increased bone mass in von Kossa–stained sections of the vertebrae and tibiae after 1 week of transgene activation (Fig. 8A). Histomorphometric quantification confirmed that *Lrp5*-deficient *Wnt1*-overexpressing mice had increased bone mass and higher trabecular numbers in both vertebrae and tibiae compared to $Lrp5^{-/-}$ mice (Fig. 8, B and C). As previously found, Wnt1 activation did not affect osteoclast parameters (Fig. 8D) but rather resulted in increased osteoblast numbers and surface area (Fig. 8E). To further confirm the Lrp5-independent bone-anabolic function of Wnt1, we calculated the net increase in bone mass when activating Wnt1 for 1 and 3 weeks in the two models (Lrp5-expressing or Lrp5-deficient mice). These calculations demonstrated that, regardless of the expression of Lrp5, Wnt1 induction caused a similar increase in BV/TV (Fig. 8F), cortical thickness (Fig. 8G), and BFR (Fig. 8H) in the two mouse

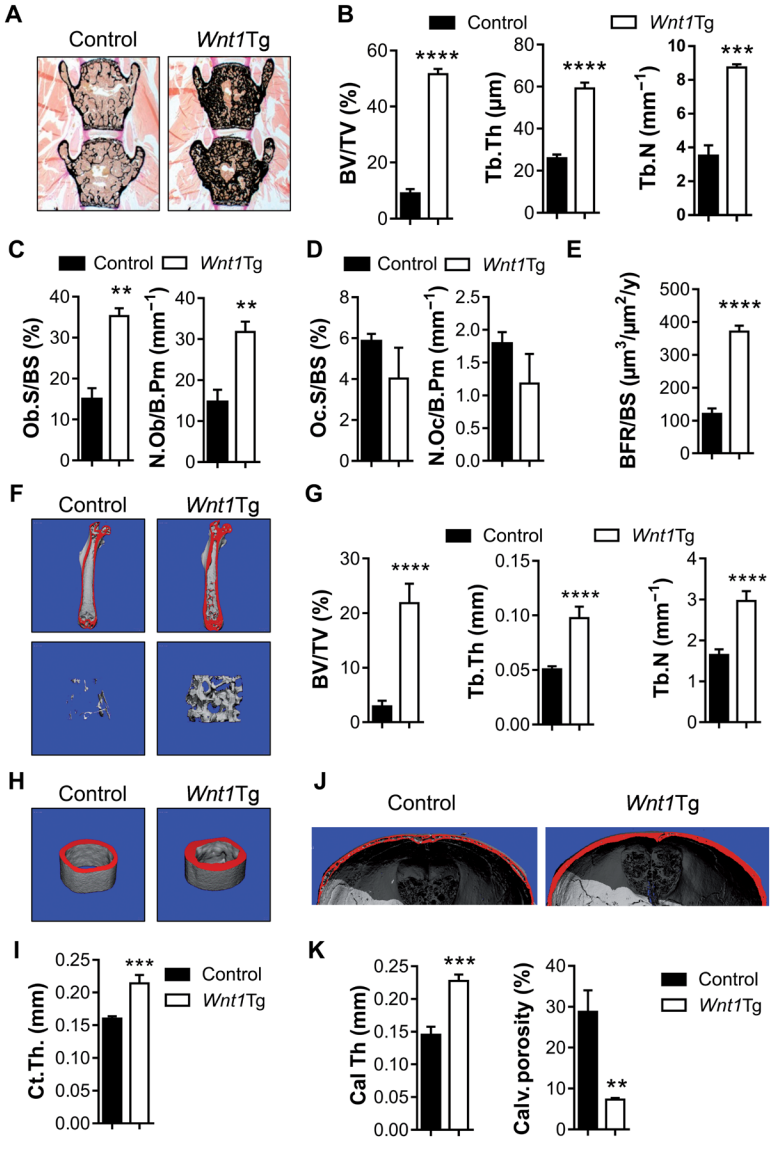

Fig. 6. *Wnt1* induces bone formation in aging mice. (**A**) von Kossa staining of sections of vertebra of 1-year-old mice maintained for 9 weeks with DOX-free food. (**B**) Histomorphometric analysis of the bone parameters (BV/TV, Tb.Th, and Tb.N). (**C**) Histomorphometric quantification of osteoblast surface area and number and (**D**) of osteoclast surface area and number. (**E**) Quantification of the BFR in the spine of the mice. BS, bone surface area. (**F**) µCT imaging of the femora, longitudinal section, and detail of the trabecular bone. (**G**) µCT quantification of the endochondral BV/TV, the trabecular thickness, and the trabecular number. (**H**) µCT imaging of transversal section at the midshaft of the femur. (**I**) Quantification of the cortical thickness in (H). (**J**) µCT imaging of the calvaria. (**K**) Quantification of the calvarial thickness (Calv.) and porosity (Calv. porosity). $n \geq 3$ (B to E), $n \geq 8$ (G and I), and $n \geq 7$ (K). Data are the means ± SEM. ****$P < 0.0001$; ***$P < 0.001$; **$P < 0.01$ (unpaired t test).

lines, supporting our hypothesis that Wnt1-mediated bone-anabolic function does not require Lrp5 co-receptor expression.

DISCUSSION

A role for WNT1 as a Wnt ligand regulating bone mass has been proposed on the basis of the low bone mass mutations identified in humans. Here, we demonstrated that Wnt1 regulates bone homeostasis in mice as a major bone-anabolic Wnt ligand produced by the osteoblast lineage. We also demonstrated that Wnt1 does not require the co-receptor Lrp5 for stimulating bone formation.

Although the role for WNT signaling in the regulation of bone resorption and bone formation is widely accepted (*3*, *36*), none of the 19 Wnt ligands [with the exception of Wnt7b, which appeared to regulate bone formation during development (*20*)] were previously identified as a bone-anabolic ligand. The potential bone-anabolic function of Wnt ligands can be deduced from indirect evidence drawn from the analysis of gain or loss of function of potential receptors, co-receptors (Lrp5 and Lrp6), inhibitors of WNT signaling [Sost and secreted frizzled-related proteins (Sfrps)], proteins involved in Wnt-ligand processing such as Wntless, or downstream transcriptional regulators, mainly β-catenin (*3*, *36*). With the exception of Wnt5a, which regulates both bone resorption and bone formation (*21*), other Wnt ligands acting on the bone, such as Wnt4 and Wnt16, directly or indirectly inhibit osteoclast differentiation or function to decrease bone resorption (*20*, *37*). Another Wnt ligand identified as a putative bone-anabolic molecule in mice is Wnt10b; genetic inactivation resulted in low bone mass, whereas overexpression in mesenchymal bone marrow protected against aging-induced bone loss. However, none of the bone phenotypes observed in the *Wnt10b*-deficient mice or in the mice overexpressing *Wnt10b* in osteoblast were distinctly attributed to variation in bone formation (*38*). The only WNT ligand associated with decreased bone mass when mutated in humans is WNT1 (*22*–*24*). In addition, a reduced bone volume due to decreased bone formation was also reported by skeletal analysis of the Swaying mouse (carrying a stop mutation that causes the expression of a shorter Wnt1 protein), thus confirming the role of Wnt1 in regulating bone formation (*25*); however, this work did not allow the identification of the cellular source of Wnt1 nor did it address its relation to Lrp5.

In a recent paper, osteocytes were proposed as a potential cellular source of Wnt1 regulating bone mass (*26*). These data were based on a mouse phenotype with Cre-mediated inactivation of Wnt1 directed by the *Dmp1* promoter to specifically target gene recombination in osteocytes. However, the osteocyte-restricted expression of Cre recombinase in this mouse line is not established, and the efficacy of recombination in this paper was not directly validated but rather indirectly assessed via recombination of a Cre-dependent reporter gene (*26*). By validating the recombination in *Dmp1-Cre;Wnt1*$^{fl/fl}$ mice, we found Cre-mediated recombination in several other tissues in addition to the bone, such as the brain, white adipose tissue, testis, and the gastrointestinal (GI) tract, confirming off-target recombination events already reported by others (*27*). Because of this broad recombination activity including the GI tract [which has been controversially proposed to mediate the WNT-signaling effect on the bone (*27*, *39*)], it is difficult to attempt to establish the cellular origin of Wnt1 function in the bone using this model. In contrast, unspecific recombination was not observed when using the *Runx2-Cre* line to mediate Wnt1 inactivation. In addition, our immunostaining on bone sections from wild-type mice indicated that bone lining cells rather than

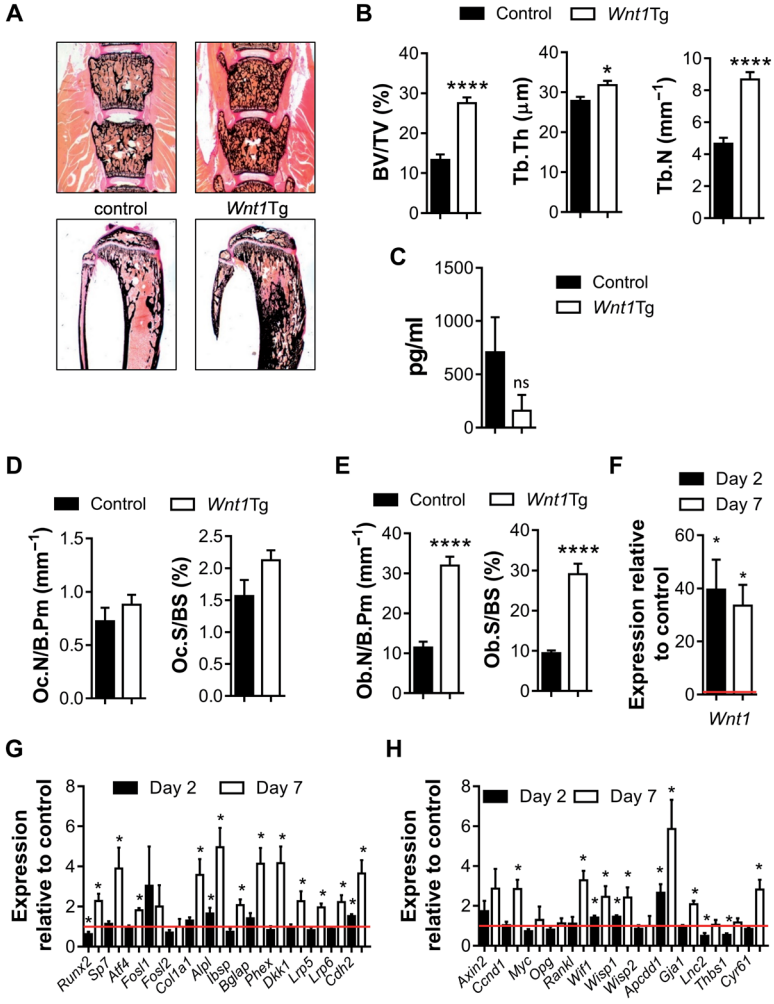

Fig. 7. The bone-anabolic effect of Wnt1 is rapid. (**A**) von Kossa staining of sections of vertebrae (top) and tibiae (bottom) of 6-week-old *Wnt1* transgenic male mice maintained for 1 week with DOX-free food. (**B**) Histomorphometric analysis of the bone parameters (BV/TV, Tb.Th, and Tb.N). $n \geq 6$. (**C**) ELISA quantification of circulating Wnt1. $n = 3$. (**D**) Quantification of osteoclast number and osteoclast surface area and (**E**) of osteoblast number and osteoblast surface area. $n \geq 5$. (**F**) QPCR analysis of the transgene expression in the calvaria of the *Wnt1*Tg mice 2 and 7 days after removing DOX; data are normalized to the control mice (red line). (**G**) QPCR analysis of the expression of markers of bone formation and (**H**) of potential Wnt/β-catenin target genes in the calvaria of the *Wnt1*Tg mice 2 and 7 days after removing DOX, normalized to control mice (red line). $n \geq 6$ (F to H). Data are the means ± SEM. $^{****}P < 0.0001$; $^{*}P < 0.05$ [unpaired *t* test (B to F) or one-sample *t* test (hypothetical value, 1; $^{*}P < 0.05$; G and H)].

bone-embedded osteocytes were expressing Wnt1. Although osteocyte markers were induced in primary culture of wild-type osteoblast induced to differentiate in vitro, no parallel time-dependent up-regulation of Wnt1 was observed. Thus, although our data do not completely exclude the possibility of Wnt1 expression in osteocytes, our findings do not favor an osteocyte-specific expression of Wnt1 as mediator of increased bone mass.

By selectively deleting *Wnt1* in osteoblasts or in osteoclasts, we provide evidence that expression of Wnt1 in the osteoblastic lineage is required for its bone-anabolic action. Several lines of evidence suggest that Wnt1, when produced by osteoblasts, might not stimulate bone formation via secretion. Deleting Wnt1 in the osteoblast lineage did not affect Wnt1 concentration in serum; although we observed a time-dependent increase in circulating Wnt1 when inducing the transgene for 3 and 9 weeks, no change was detected after 1 week of induction, a time point when the bone phenotype is already evident. These observations exclude a systemic effect of Wnt1 that may have resulted from its increased expression in the spleen of the transgenic mice. Despite increased expression of Wnt1 protein in primary osteoblast isolated from the transgenic mice, Wnt1 was not detected in the supernatant of the cell culture. In contrast to the reported increased differentiation upon Wnt1 overexpression in the ST2 cell line via mTORC1 pathway activation (*26*), Wnt1 overexpression in primary osteoblasts did not directly activate osteoblast differentiation nor increase S6 phosphorylation, despite the evidence for some autocrine effect as shown by the repression of *Bglap* and the stimulation of *Apcdd1* expression. Thus, our work supports a general model postulating a short range of action for Wnt ligands (*3*). In agreement, we proposed that Wnt1 produced by osteoblasts acts in a juxtacrine manner to stimulate bone formation.

Using a conditional inducible gain-of-function model, our work demonstrates that Wnt1 activation in osteoblasts promotes a robust increase in bone mass caused by increased bone formation under all conditions tested (growing, adult, and aging mice). This effect is gender independent and affects all types of bones: trabecular, cortical, and intramembranous bone. Mechanistically, this effect is directly linked to increased osteoblast numbers and does not affect bone resorption. Most surprising was the speed of this process documented by the pronounced increase in bone mass after a single week of transgene induction. Therefore, we believe that Wnt1 is a potent stimulator of bone formation and that pharmacological agonists mimicking Wnt1 function will have utility for treating low bone mass syndromes. However, caution should be taken when developing agonistic molecules: The WNT pathways are known to be involved in numerous human pathologies. In particular, Wnt1 was originally identified as an oncogene inducing breast tumors in mice (*40*). In this regard, the effects and possible deleterious consequences arising during long-term Wnt1 expression require further investigation.

Another important finding of our work is that Wnt1 does not require the expression of Lrp5 to exert its bone-anabolic function, as shown by Wnt1 transgene expression in *Lrp5*-deficient mice. In the absence of Lrp5, the net-increased bone mass observed when inducing Wnt1 was similar to the observed bone mass increase in the wild-type mice. This increased bone mass was caused by a similar increase in BFRs, and increased bone mass in *Lrp5*-deficient *Wnt1*Tg mice thus demonstrates that both pathways act independently to regulate bone formation without compensatory effects mediated by Lrp6. This was unexpected, given the high bone mass phenotype observed in mice and humans with Lrp5 gain-of-function mutations (*33*, *34*, *41*, *42*). This discrepancy cannot be explained by a redundant function of Lrp5 and Lrp6 as described for the GI tract development (*43*) as well as for Wnt-induced bone development and formation (*44*–*47*). Whether Wnt1 is mainly acting via Lrp6 in the bone is an appealing hypothesis suggested by the Sost deficiency–mediated increased bone mass still observed in

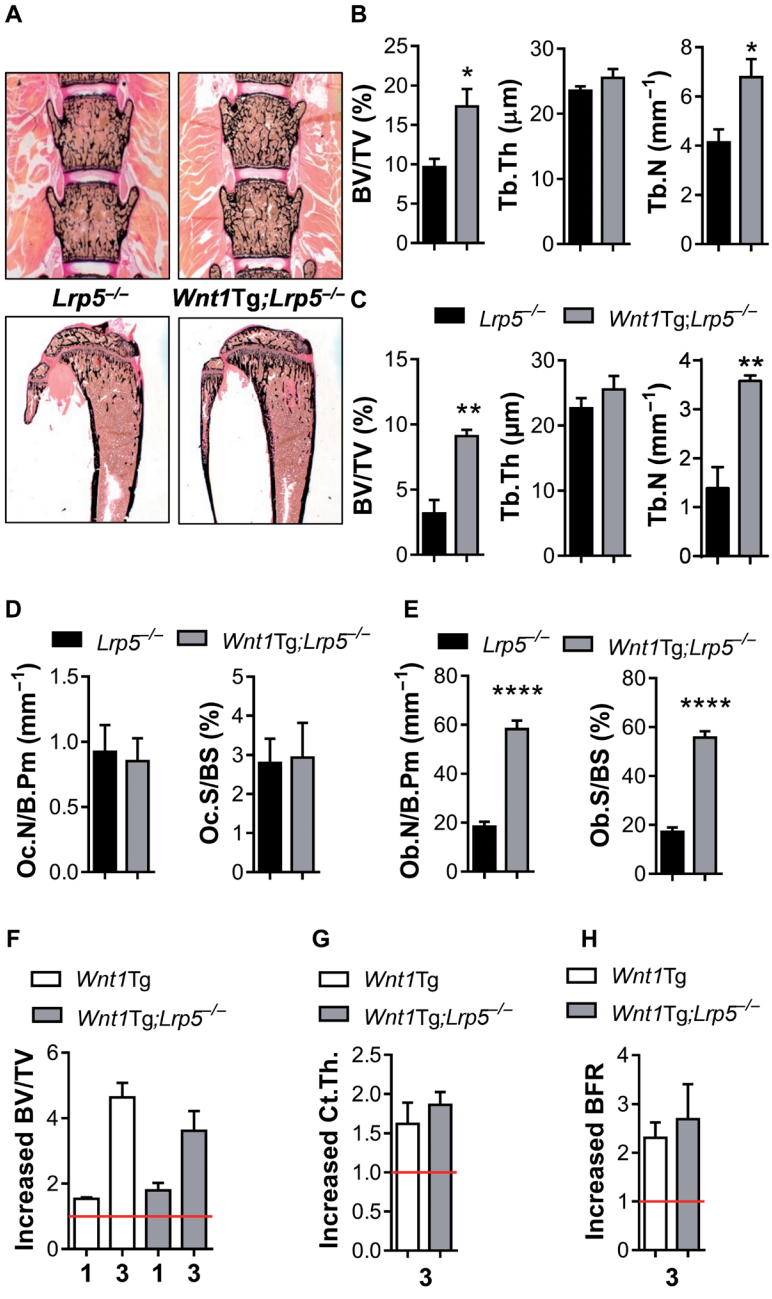

Fig. 8. The bone-anabolic effect of Wnt1 is independent of Lrp5. (**A**) von Kossa staining of sections of vertebrae and tibiae of 6-week-old male mice maintained for 1 week with DOX-free food. (**B**) Histomorphometric analysis of the bone parameters (BV/TV, Tb.Th, and Tb.N) in the vertebrae and (**C**) in the tibiae. (**D**) Quantification of osteoclast number and osteoclast surface area and (**E**) of osteoblast number and osteoblast surface area in the vertebrae. (**F**) Comparison of the BV/TV between *Wnt1*Tg and *Wnt1*Tg;*Lrp5*$^{-/-}$ mice 1 and 3 weeks after removing the DOX. (**G**) Comparison of the increased cortical thickness 3 weeks after removing the DOX. (**H**) Comparison of the BFR 3 weeks after removing the DOX. The values in (F), (G) and (H) are reported as fold changes of their respective controls (red lines, nontransgenic or *Lrp5*$^{-/-}$ mice). $n = 5$ (B, D, and E), $n \geq 3$ (C, F, and H), $n \geq 4$ (G). Data are the means ± SEM. ****$P < 0.0001$; **$P < 0.01$; *$P < 0.05$ (unpaired t test).

Lrp5-deficient mice that could be reversed by treatment with specific Wnt1 class–mediated Lrp6-signaling blocking antibody (*46*, *48*). This hypothesis remains to be tested. The Lrp5-independent regulation of bone formation by Wnt1 also raises the question of the identity of the frizzled receptor involved in both cases, as well as of the WNT pathway (canonical or noncanonical). Although it is widely believed that Lrp5 is mediating a canonical WNT signaling response, the only Wnt receptor with a known bone-anabolic function identified to date is Fzd9, which acts through the WNT noncanonical pathway (*19*), as does Wnt7b (*20*). Although our in vivo gene expression analysis suggested that Wnt1 would act as a canonical rather than a noncanonical Wnt ligand, whether Fzd9 is required or at least partly involved in mediating Wnt1 action in bone needs further investigation.

The main limitation of our study is that, although we clearly demonstrated the bone-anabolic function of Wnt1, we did not address the mechanism underlying the bone phenotypes caused by WNT1 mutations in humans, which would require generating mouse models carrying similar mutations. A second limitation of the work is whether switching on WNT1 signaling could lead to any deleterious side effect that was not addressed. These points are essential to test the efficacy of any therapies involving WNT1 agonist.

To date, the PTHR (PTH receptor) agonists teriparatide and abaloparatide are the only approved bone-anabolic treatment, and all new drugs under development are targeting the activation of the WNT-LRP5 pathway. Teriparatide had the potential to improve the bone status of a patient carrying a *WNT1* mutation, therefore bypassing the WNT1 loss of function in bone, directly confirming an observation previously reported by others (*49*). When combined with the identification of Wnt1 as an efficient regulator of bone formation that acts independently of Lrp5 in bone, these observations demonstrate that multiple bone-anabolic pathways could be sequentially targeted to stimulate bone formation, thereby limiting the risk of side effects upon long-term treatment. Thus, the discovery of Wnt1 as an Lrp5-independent regulator of bone formation provides the basis for a novel class of drugs targeting low bone mass pathologies.

MATERIALS AND METHODS

Study design

The objective of this study was to determine the function of Wnt1 in bone homeostasis. Because *WNT1* mutations in humans are associated with bone disorders, we analyzed the prevalence of heterozygous *WNT1* mutations in patients with early-onset osteoporosis. Informed consent was obtained from all patients for the presented data. The study was approved by the Ethics Committee of the Hamburg Chamber of Physicians (agreement number PV 5364). Using mouse models, we analyzed the effect of monocyte- or osteoblast-specific Wnt1 inactivation and osteoblast-targeted overexpression on bone formation and remodeling and investigated whether Wnt1 function requires the expression of the known bone-anabolic co-receptor Lrp5 by crossing the *Wnt1*Tg mouse with an *Lrp5*ko mouse. Samples were assigned randomly to the experimental groups. For animal studies, littermates were used as control. Sample size was determined by availability; for most experiments, at least three samples were analyzed in a blinded fashion. For cell culture, three independent experiments

were performed. Outliers were identified by robust regression and outlier removal (ROUT) method using GraphPad Prism.

Statistical analysis

The data were analyzed using GraphPad Prism software (GraphPad Software Inc.) and are reported as means ± SEM. Unpaired *t* test or one-sample *t* test with a hypothetical value of 1 when comparing two groups and one-way ANOVA with Bonferroni's comparisons test when comparing multiple groups was used to determine the statistical significance [$*P < 0.05$; $**P < 0.01$; $***P < 0.001$; $****P < 0.0001$ (unpaired *t* test or one-way ANOVA) or $*P < 0.05$ (one-sample *t* test)].

SUPPLEMENTARY MATERIALS

www.sciencetranslationalmedicine.org/cgi/content/full/10/466/eaau7137/DC1
Materials and Methods
Fig. S1. Age-related decreased bone mass in the radius of patients with WNT1 mutation.
Fig. S2. Inactivation of Wnt1 in osteoclasts does not affect bone remodeling.
Fig. S3. Histology of the fractures in *Runx2-cre;Wnt1*$^{fl/fl}$ mice.
Fig. S4. Wnt1 is a general bone-anabolic molecule.
Fig. S5. Wnt1 induces bone formation in adult mice.
Fig. S6. Wnt1 induction protects aging female from bone loss.
Fig. S7. Wnt1 expression induces a rapidly increased bone mass in adult mice.
Fig. S8. Wnt1 is not directly stimulating osteoblast differentiation.
Fig. S9. Wnt1 is not up-regulated during osteoblast differentiation.
Table S1. Individual subject-level data (Excel file).
References (*50*–*58*)

REFERENCES AND NOTES

1. G. Schett, J.-P. David, The multiple faces of autoimmune-mediated bone loss. *Nat. Rev. Endocrinol.* **6**, 698–706 (2010).
2. T. A. Yorgan, T. Schinke, Relevance of Wnt signaling for osteoanabolic therapy. *Mol. Cell. Ther.* **2**, 22 (2014).
3. R. Baron, M. Kneissel, WNT signaling in bone homeostasis and disease: From human mutations to treatments. *Nat. Med.* **19**, 179–192 (2013).
4. T. D. Rachner, S. Khosla, L. C. Hofbauer, Osteoporosis: Now and the future. *Lancet* **377**, 1276–1287 (2011).
5. B. Langdahl, S. Ferrari, D. W. Dempster, Bone modeling and remodeling: Potential as therapeutic targets for the treatment of osteoporosis. *Ther. Adv. Musculoskelet. Dis.* **8**, 225–235 (2016).
6. J. S. Chen, P. N. Sambrook, Antiresorptive therapies for osteoporosis: A clinical overview. *Nat. Rev. Endocrinol.* **8**, 81–91 (2012).
7. S. Teufel, B. Grötsch, J. Luther, A. Derer, T. Schinke, M. Amling, G. Schett, D. Mielenz, J.-P. David, Inhibition of bone remodeling in young mice by bisphosphonate displaces the plasma cell niche into the spleen. *J. Immunol.* **193**, 223–233 (2014).
8. J. P. Brown, S. Morin, W. Leslie, A. Papaioannou, A. M. Cheung, K. S. Davison, D. Goltzman, D. A. Hanley, A. Hodsman, R. Josse, A. Jovaisas, A. Juby, S. Kaiser, A. Karaplis, D. Kendler, A. Khan, D. Ngui, W. Olszynski, L.-G. Ste-Marie, J. Adachi, Bisphosphonates for treatment of osteoporosis: Expected benefits, potential harms, and drug holidays. *Can. Fam. Physician* **60**, 324–333 (2014).
9. A. Mansour, A. Anginot, S. J. C. Mancini, C. Schiff, G. F. Carle, A. Wakkach, C. Blin-Wakkach, Osteoclast activity modulates B-cell development in the bone marrow. *Cell Res.* **21**, 1102–1115 (2011).
10. R. M. Neer, C. D. Arnaud, J. R. Zanchetta, R. Prince, G. A. Gaich, J.-Y. Reginster, A. B. Hodsman, E. F. Eriksen, S. Ish-Shalom, H. K. Genant, O. Wang, D. Mellström, E. S. Oefjord, E. Marcinowska-Suchowierska, J. Salmi, H. Mulder, J. Halse, A. Z. Sawicki, B. H. Mitlak, Effect of parathyroid hormone (1-34) on fractures and bone mineral density in postmenopausal women with osteoporosis. *N. Engl. J. Med.* **344**, 1434–1441 (2001).
11. J. L. Vahle, M. Sato, G. G. Long, J. K. Young, P. C. Francis, J. A. Engelhardt, M. S. Westmore, Y. Linda, J. B. Nold, Skeletal changes in rats given daily subcutaneous injections of recombinant human parathyroid hormone (1–34) for 2 years and relevance to human safety. *Toxicol. Pathol.* **30**, 312–321 (2002).
12. D. M. Joiner, J. Ke, Z. Zhong, H. E. Xu, B. O. Williams, LRP5 and LRP6 in development and disease. *Trends Endocrinol. Metab.* **24**, 31–39 (2013).
13. W. Balemans, M. Ebeling, N. Patel, E. Van Hul, P. Olson, M. Dioszegi, C. Lacza, W. Wuyts, J. Van Den Ende, P. Willems, A. F. Paes-Alves, S. Hill, M. Bueno, F. J. Ramos, P. Tacconi, F. G. Dikkers, C. Stratakis, K. Lindpaintner, B. Vickery, D. Foernzler, W. Van Hul, Increased bone density in sclerosteosis is due to the deficiency of a novel secreted protein (SOST). *Hum. Mol. Genet.* **10**, 537–544 (2001).
14. T. F. Day, X. Guo, L. Garrett-Beal, Y. Yang, Wnt/β-catenin signaling in mesenchymal progenitors controls osteoblast and chondrocyte differentiation during vertebrate skeletogenesis. *Dev. Cell* **8**, 739–750 (2005).
15. T. P. Hill, D. Später, M. M. Taketo, W. Birchmeier, C. Hartmann, Canonical Wnt/β-catenin signaling prevents osteoblasts from differentiating into chondrocytes. *Dev. Cell* **8**, 727–738 (2005).
16. D. A. Glass II, P. Bialek, J. D. Ahn, M. Starbuck, M. S. Patel, H. Clevers, M. M. Taketo, F. Long, A. P. McMahon, R. A. Lang, G. Karsenty, Canonical Wnt signaling in differentiated osteoblasts controls osteoclast differentiation. *Dev. Cell* **8**, 751–764 (2005).
17. J. Albers, J. Keller, A. Baranowsky, F. T. Beil, P. Catala-Lehnen, J. Schulze, M. Amling, T. Schinke, Canonical Wnt signaling inhibits osteoclastogenesis independent of osteoprotegerin. *J. Cell Biol.* **200**, 537–549 (2013).
18. C. Scholtysek, J. Katzenbeisser, H. Fu, S. Uderhardt, N. Ipseiz, C. Stoll, M. M. Zaiss, M. Stock, L. Donhauser, C. Böhm, A. Kleyer, A. Hess, K. Engelke, J.-P. David, F. Djouad, J. P. Tuckermann, B. Desvergne, G. Schett, G. Krönke, PPARβ/δ governs Wnt signaling and bone turnover. *Nat. Med.* **19**, 608–613 (2013).
19. J. Albers, J. Schulze, F. T. Beil, M. Gebauer, A. Baranowsky, J. Keller, R. P. Marshall, K. Wintges, F. W. Friedrich, M. Priemel, A. F. Schilling, J. M. Rueger, K. Cornils, B. Fehse, T. Streichert, G. Sauter, F. Jakob, K. L. Insogna, B. Pober, K.-P. Knobeloch, U. Francke, M. Amling, T. Schinke, Control of bone formation by the serpentine receptor Frizzled-9. *J. Cell Biol.* **192**, 1057–1072 (2011).
20. X. Tu, K. S. Joeng, K. I. Nakayama, K. Nakayama, J. Rajagopal, T. J. Carroll, A. P. McMahon, F. Long, Noncanonical Wnt signaling through G protein-linked PKCδ activation promotes bone formation. *Dev. Cell* **12**, 113–127 (2007).
21. K. Maeda, Y. Kobayashi, N. Udagawa, S. Uehara, A. Ishihara, T. Mizoguchi, Y. Kikuchi, I. Takada, S. Kato, S. Kani, M. Nishita, K. Marumo, T. J. Martin, Y. Minami, N. Takahashi, Wnt5a-Ror2 signaling between osteoblast-lineage cells and osteoclast precursors enhances osteoclastogenesis. *Nat. Med.* **18**, 405–412 (2012).
22. C. M. Laine, K. S. Joeng, P. M. Campeau, R. Kiviranta, K. Tarkkonen, M. Grover, J. T. Lu, M. Pekkinen, M. Wessman, T. J. Heino, V. Nieminen-Pihala, M. Aronen, T. Laine, H. Kröger, W. G. Cole, A.-E. Lehesjoki, L. Nevarez, D. Krakow, C. J. R. Curry, D. H. Cohn, R. A. Gibbs, B. H. Lee, O. Mäkitie, *WNT1* mutations in early-onset osteoporosis and osteogenesis imperfecta. *N. Engl. J. Med.* **368**, 1809–1816 (2013).
23. K. Keupp, F. Beleggia, H. Kayserili, A. M. Barnes, M. Steiner, O. Semler, B. Fischer, G. Yigit, C. Y. Janda, J. Becker, S. Breer, U. Altunoglu, J. Grünhagen, P. Krawitz, J. Hecht, T. Schinke, E. Makareeva, E. Lausch, T. Cankaya, J. A. Caparrós-Martin, P. Lapunzina, S. Temtamy, M. Aglan, B. Zabel, P. Eysel, F. Koerber, S. Leikin, K. C. Garcia, C. Netzer, E. Schönau, V. L. Ruiz-Perez, S. Mundlos, M. Amling, U. Kornak, J. Marini, B. Wollnik, Mutations in *WNT1* cause different forms of bone fragility. *Am. J. Hum. Genet.* **92**, 565–574 (2013).
24. S. Fahiminiya, J. Majewski, J. Mort, P. Moffatt, F. H. Glorieux, F. Rauch, Mutations in WNT1 are a cause of osteogenesis imperfecta. *J. Med. Genet.* **50**, 345–348 (2013).
25. K. S. Joeng, Y.-C. Lee, M.-M. Jiang, T. K. Bertin, Y. Chen, A. M. Abraham, H. Ding, X. Bi, C. G. Ambrose, B. H. Lee, The swaying mouse as a model of osteogenesis imperfecta caused by *WNT1* mutations. *Hum. Mol. Genet.* **23**, 4035–4042 (2014).
26. K. S. Joeng, Y.-C. Lee, J. Lim, Y. Chen, M.-M. Jiang, E. Munivez, C. Ambrose, B. H. Lee, Osteocyte-specific WNT1 regulates osteoblast function during bone homeostasis. *J. Clin. Invest.* **127**, 2678–2688 (2017).
27. Y. Cui, P. J. Niziolek, B. T. MacDonald, C. R. Zylstra, N. Alenina, D. R. Robinson, Z. Zhong, S. Matthes, C. M. Jacobsen, R. A. Conlon, R. Brommage, Q. Liu, F. Mseeh, D. R. Powell, Q. M. Yang, B. Zambrowicz, H. Gerrits, J. A. Gossen, X. He, M. Bader, B. O. Williams, M. L. Warman, A. G. Robling, Lrp5 functions in bone to regulate bone mass. *Nat. Med.* **17**, 684–691 (2011).
28. H. M. Macdonald, K. K. Nishiyama, J. Kang, D. A. Hanley, S. K. Boyd, Age-related patterns of trabecular and cortical bone loss differ between sexes and skeletal sites: A population-based HR-pQCT study. *J. Bone Miner. Res.* **26**, 50–62 (2011).
29. L. A. Burt, Z. Liang, T. T. Sajobi, D. A. Hanley, S. K. Boyd, Sex- and site-specific normative data curves for HR-pQCT. *J. Bone Miner. Res.* **31**, 2041–2047 (2016).
30. M. M. Weivoda, M. Ruan, L. Pederson, C. Hachfeld, R. A. Davey, J. D. Zajac, J. J. Westendorf, S. Khosla, M. J. Oursler, Osteoclast TGF-β receptor signaling induces Wnt1 secretion and couples bone resorption to bone formation. *J. Bone Miner. Res.* **31**, 76–85 (2016).
31. Y. Shimomura, D. Agalliu, A. Vonica, V. Luria, M. Wajid, A. Baumer, S. Belli, L. Petukhova, A. Schinzel, A. H. Brivanlou, B. A. Barres, A. M. Christiano, APCDD1 is a novel Wnt inhibitor mutated in hereditary hypotrichosis simplex. *Nature* **464**, 1043–1047 (2010).
32. R. A. Kahler, J. J. Westendorf, Lymphoid enhancer factor-1 and β-catenin inhibit Runx2-dependent transcriptional activation of the osteocalcin promoter. *J. Biol. Chem.* **278**, 11937–11944 (2003).

33. L. M. Boyden, J. Mao, J. Belsky, L. Mitzner, A. Farhi, M. A. Mitnick, D. Wu, K. Insogna, R. P. Lifton, High bone density due to a mutation in LDL-receptor–related protein 5. *N. Engl. J. Med.* **346**, 1513–1521 (2002).
34. P. Babij, W. Zhao, C. Small, Y. Kharode, P. J. Yaworsky, M. L. Bouxsein, P. S. Reddy, P. V. Bodine, J. A. Robinson, B. Bhat, J. Marzolf, R. A. Moran, F. Bex, High bone mass in mice expressing a mutant *LRP5* gene. *J. Bone Miner. Res.* **18**, 960–974 (2003).
35. M. Kato, M. S. Patel, R. Levasseur, I. Lobov, B. H.-J. Chang, D. A. Glass II, C. Hartmann, L. Li, T.-H. Hwang, C. F. Brayton, R. A. Lang, G. Karsenty, L. Chan, *Cbfa1*-independent decrease in osteoblast proliferation, osteopenia, and persistent embryonic eye vascularization in mice deficient in Lrp5, a Wnt coreceptor. *J. Cell Biol.* **157**, 303–314 (2002).
36. B. O. Williams, Genetically engineered mouse models to evaluate the role of Wnt secretion in bone development and homeostasis. *Am. J. Med. Genet. C Semin. Med. Genet.* **172**, 24–26 (2016).
37. B. Yu, J. Chang, Y. Liu, J. Li, K. Kevork, K. Al-Hezaimi, D. T. Graves, N.-H. Park, C.-Y. Wang, Wnt4 signaling prevents skeletal aging and inflammation by inhibiting nuclear factor-κB. *Nat. Med.* **20**, 1009–1017 (2014).
38. C. N. Bennett, K. A. Longo, W. S. Wright, L. J. Suva, T. F. Lane, K. D. Hankenson, O. A. MacDougald, Regulation of osteoblastogenesis and bone mass by Wnt10b. *Proc. Natl. Acad. Sci. U.S.A.* **102**, 3324–3329 (2005).
39. V. K. Yadav, J.-H. Ryu, N. Suda, K. F. Tanaka, J. A. Gingrich, G. Schütz, F. H. Glorieux, C. Y. Chiang, J. D. Zajac, K. L. Insogna, J. J. Mann, R. Hen, P. Ducy, G. Karsenty, Lrp5 controls bone formation by inhibiting serotonin synthesis in the duodenum: An entero-bone endocrine axis. *Cell* **135**, 825–837 (2008).
40. R. Nusse, H. E. Varmus, Many tumors induced by the mouse mammary tumor virus contain a provirus integrated in the same region of the host genome. *Cell* **31**, 99–109 (1982).
41. L. Van Wesenbeeck, E. Cleiren, J. Gram, R. K. Beals, O. Benichou, D. Scopelliti, L. Key, T. Renton, C. Bartels, Y. Gong, M. L. Warman, M. C. De Vernejoul, J. Bollerslev, W. Van Hul, Six novel missense mutations in the LDL receptor-related protein 5 (LRP5) gene in different conditions with an increased bone density. *Am. J. Hum. Genet.* **72**, 763–771 (2003).
42. R. D. Little, J. P. Carulli, R. G. Del Mastro, J. Dupuis, M. Osborne, C. Folz, S. P. Manning, P. M. Swain, S.-C. Zhao, B. Eustace, M. M. Lappe, L. Spitzer, S. Zweier, K. Braunschweiger, Y. Benchekroun, X. Hu, R. Adair, L. Chee, M. G. FitzGerald, C. Tulig, A. Caruso, N. Tzellas, A. Bawa, B. Franklin, S. McGuire, X. Nogues, G. Gong, K. M. Allen, A. Anisowicz, A. J. Morales, P. T. Lomedico, S. M. Recker, P. Van Eerdewegh, R. R. Recker, M. L. Johnson, A mutation in the LDL receptor-related protein 5 gene results in the autosomal dominant high-bone-mass trait. *Am. J. Hum. Genet.* **70**, 11–19 (2002).
43. Z. Zhong, J. J. Baker, C. R. Zylstra-Diegel, B. O. Williams, Lrp5 and Lrp6 play compensatory roles in mouse intestinal development. *J. Cell. Biochem.* **113**, 31–38 (2012).
44. S. L. Holmen, T. A. Giambernardi, C. R. Zylstra, B. D. Buckner-Berghuis, J. H. Resau, J. F. Hess, V. Glatt, M. L. Bouxsein, M. Ai, M. L. Warman, B. O. Williams, Decreased BMD and limb deformities in mice carrying mutations in both *Lrp5* and *Lrp6*. *J. Bone Miner. Res.* **19**, 2033–2040 (2004).
45. K. S. Joeng, C. A. Schumacher, C. R. Zylstra-Diegel, F. Long, B. O. Williams, Lrp5 and Lrp6 redundantly control skeletal development in the mouse embryo. *Dev. Biol.* **359**, 222–229 (2011).
46. R. Kedlaya, S. Veera, D. J. Horan, R. E. Moss, U. M. Ayturk, C. M. Jacobsen, M. E. Bowen, C. Paszty, M. L. Warman, A. G. Robling, Sclerostin inhibition reverses skeletal fragility in an Lrp5-deficient mouse model of OPPG syndrome. *Sci. Transl. Med.* **5**, 211ra158 (2013).
47. R. C. Riddle, C. R. Diegel, J. M. Leslie, K. K. Van Koevering, M. C. Faugere, T. L. Clemens, B. O. Williams, Lrp5 and Lrp6 exert overlapping functions in osteoblasts during postnatal bone acquisition. *PLOS ONE* **8**, e63323 (2013).
48. M.-K. Chang, I. Kramer, H. Keller, J. H. Gooi, C. Collett, D. Jenkins, S. A. Ettenberg, F. Cong, C. Halleux, M. Kneissel, Reversing *LRP5*-dependent osteoporosis and *SOST* deficiency-induced sclerosing bone disorders by altering WNT signaling activity. *J. Bone Miner. Res.* **29**, 29–42 (2014).
49. V. V. Välimäki, O. Mäkitie, R. Pereira, C. Laine, K. Wesseling-Perry, J. Määttä, M. Kirjavainen, H. Viljakainen, M. J. Välimäki, Teriparatide treatment in patients with *WNT1* or *PLS3* mutation-related early-onset osteoporosis: A pilot study. *J. Clin. Endocrinol. Metab.* **102**, 535–544 (2016).
50. P. Milovanovic, U. Adamu, M. J. Simon, T. Rolvien, M. Djuric, M. Amling, B. Busse, Age- and sex-specific bone structure patterns portend bone fragility in radii and tibiae in relation to osteodensitometry: A high-resolution peripheral quantitative computed tomography study in 385 individuals. *J. Gerontol. A Biol. Sci. Med. Sci.* **70**, 1269–1275 (2015).
51. M. Priemel, C. von Domarus, T. O. Klatte, S. Kessler, J. Schlie, S. Meier, N. Proksch, F. Pastor, C. Netter, T. Streichert, K. Püschel, M. Amling, Bone mineralization defects and vitamin D deficiency: Histomorphometric analysis of iliac crest bone biopsies and circulating 25-hydroxyvitamin D in 675 patients. *J. Bone Miner. Res.* **25**, 305–312 (2010).
52. D. W. Dempster, J. E. Compston, M. K. Drezner, F. H. Glorieux, J. A. Kanis, H. Malluche, P. J. Meunier, S. M. Ott, R. R. Recker, A. M. Parfitt, Standardized nomenclature, symbols, and units for bone histomorphometry: A 2012 update of the report of the ASBMR Histomorphometry Nomenclature Committee. *J. Bone Miner. Res.* **28**, 2–17 (2013).
53. J. N. Tsai, A. V. Uihlein, H. Lee, R. Kumbhani, E. Siwila-Sackman, E. A. McKay, S. A. Burnett-Bowie, R. M. Neer, B. Z. Leder, Teriparatide and denosumab, alone or combined, in women with postmenopausal osteoporosis: The DATA study randomised trial. *Lancet* **382**, 50–56 (2013).
54. A. Rauch, S. Seitz, U. Baschant, A. F. Schilling, A. Illing, B. Stride, M. Kirilov, V. Mandic, A. Takacz, R. Schmidt-Ullrich, S. Ostermay, T. Schinke, R. Spanbroek, M. M. Zaiss, P. E. Angel, U. H. Lerner, J. P. David, H. M. Reichardt, M. Amling, G. Schutz, J. P. Tuckermann, Glucocorticoids suppress bone formation by attenuating osteoblast differentiation via the monomeric glucocorticoid receptor. *Cell Metab.* **11**, 517–531 (2010).
55. B. E. Clausen, C. Burkhardt, W. Reith, R. Renkawitz, I. Förster, Conditional gene targeting in macrophages and granulocytes using LysMcre mice. *Transgenic Res.* **8**, 265–277 (1999).
56. E. J. Gunther, S. E. Moody, G. K. Belka, K. T. Hahn, N. Innocent, K. D. Dugan, R. D. Cardiff, L. A. Chodosh, Impact of p53 loss on reversal and recurrence of conditional Wnt-induced tumorigenesis. *Genes Dev.* **17**, 488–501 (2003).
57. T. A. Yorgan, S. Peters, A. Jeschke, P. Benisch, F. Jakob, M. Amling, T. Schinke, The anti-osteoanabolic function of sclerostin is blunted in mice carrying a high bone mass mutation of Lrp5. *J. Bone Miner. Res.* **30**, 1175–1183 (2015).
58. W. Jochum, J.-P. David, C. Elliott, A. Wutz, H. Plenk Jr., K. Matsuo, E. F. Wagner, Increased bone formation and osteosclerosis in mice overexpressing the transcription factor Fra-1. *Nat. Med.* **6**, 980–984 (2000).

Acknowledgments: We thank I. Hermans-Borgmeyer from the mouse facility of University Medical Center Hamburg-Eppendorf for generating the conditional *Wnt1* knockout mouse line and O. Winter for technical assistance with the mouse histology. **Funding:** This work was supported by the DFG (Deutsche Forschungsgemeinschaft) grants AM103/29, DA1067/5, and SCHI 504/6 to J.-P.D., M.A., and T.S.; by the DFG Research Unit FOR 2165 to U.K.; by DIMEOS (1EC1402B) from the German Federal Ministry of Education and Research (BMBF) and the FP7-EU grant agreement number 602300 (SYBIL) to T.S., M.A., U.K., and S.M.; and by the DFG Research Unit FOR2033 Nichen consortium to A.T. **Author contributions:** J.L. performed and analyzed most of the experiments regarding the *Wnt1*Tg mice, T.A.Y. performed and analyzed the experiments regarding the *Wnt1* knockout mice, and T.R. generated and analyzed the human data; all three participated to the writing of the manuscript. L.U., D.K., and S.T. performed some of the analyses of the *Wnt1*Tg mice, and N.V. performed some of the analyses of the *Wnt1* knockout mice. T.K. and N.L. analyzed the craniofacial phenotype. M.N. and S.P. technically assisted the work. M.S. performed the immunohistology. A.T., S.R., and E.B. provided the inducible transgenic model and corrected the manuscript. S.M. and U.K. performed the genetic analysis of the mutations in patients and corrected the manuscript. R.O. and M.A. diagnosed the patients. M.A., T.S., and J.-P.D. designed and supervised the study and wrote the manuscript. **Competing interests:** The authors declare that they have no competing interests. **Data and materials availability:** All data associated with this study are present in the paper or the Supplementary Materials.

Submitted 9 July 2018
Accepted 15 October 2018
Published 7 November 2018
10.1126/scitranslmed.aau7137

Citation: J. Luther, T. A. Yorgan, T. Rolvien, L. Ulsamer, T. Koehne, N. Liao, D. Keller, N. Vollersen, S. Teufel, M. Neven, S. Peters, M. Schweizer, A. Trumpp, S. Rosigkeit, E. Bockamp, S. Mundlos, U. Kornak, R. Oheim, M. Amling, T. Schinke, J.-P. David, Wnt1 is an Lrp5-independent bone-anabolic Wnt ligand. *Sci. Transl. Med.* **10**, eaau7137 (2018).

Science Translational Medicine

Wnt1 is an Lrp5-independent bone-anabolic Wnt ligand

Julia Luther, Timur Alexander Yorgan, Tim Rolvien, Lorenz Ulsamer, Till Koehne, Nannan Liao, Daniela Keller, Nele Vollersen, Stefan Teufel, Mona Neven, Stephanie Peters, Michaela Schweizer, Andreas Trumpp, Sebastian Rosigkeit, Ernesto Bockamp, Stefan Mundlos, Uwe Kornak, Ralf Oheim, Michael Amling, Thorsten Schinke and Jean-Pierre David

Sci Transl Med **10**, eaau7137.
DOI: 10.1126/scitranslmed.aau7137

Building bone

Wnt signaling is important for proper embryonic development, shaping cell fate and migration, stem cell renewal, and organ and tissue formation. Here, Luther *et al.* investigated the role of Wnt1 in osteoporosis. Patients with early-onset osteoporosis and with *WNT1* mutations had low bone turnover and high fracture rates, and loss of Wnt1 activity caused fracture and osteoporosis in mice. Inducing Wnt1 in bone-forming cells increased bone mass in aged mice, and this process did not require Lrp5, a co-receptor involved in Wnt signaling. This study identifies Wnt1 as an anabolic (bone building) factor and suggests that it might be a therapeutic target for osteoporosis.